

Published in final edited form as:

Neuron. 2010 September 9; 67(5): 781–796. doi:10.1016/j.neuron.2010.08.008.

Global Control of Motor Neuron Topography Mediated by the Repressive Actions of a Single *Hox* Gene

Heekyung Jung^{1,6}, Julie Lacombe^{1,6}, Esteban O. Mazzoni^{2,6}, Karel F. Liem Jr^{3,6}, Jonathan Grinstein¹, Shaun Mahony⁴, Debnath Mukhopadhyay⁵, David K. Gifford⁴, Richard A. Young⁵, Kathryn V. Anderson³, Hynek Wichterle², and Jeremy S. Dasen¹

¹Howard Hughes Medical Institute Smilow Neuroscience Program Department of Physiology and Neuroscience New York University School of Medicine New York, NY 10016

²Departments of Pathology, Neurology and Neuroscience Columbia University New York, NY 10032

³Developmental Biology Program Sloan-Kettering Institute New York, NY 10021

⁴Department of Computer Science and Electrical Engineering, Massachusetts Institute of Technology, Cambridge, MA 02139

⁵Whitehead Institute for Biomedical Research, Cambridge, MA 02142

Summary

In the developing spinal cord, regional and combinatorial activities of *Hox* transcription factors are critical in controlling motor neuron fates along the rostrocaudal axis, exemplified by the precise pattern of limb innervation by more than fifty *Hox*-dependent motor pools. The mechanisms by which motor neuron diversity is constrained to limb-levels are however not well understood. We show that a single *Hox* gene, *Hoxc9*, has an essential role in organizing the motor system through global repressive activities. *Hoxc9* is required for the generation of thoracic motor columns and in its absence neurons acquire the fates of limb-innervating populations. Unexpectedly, multiple *Hox* genes are derepressed in *Hoxc9* mutants, leading to motor pool disorganization and alterations in the connections by thoracic and forelimb-level subtypes. Genome-wide analysis of *Hoxc9* binding suggests this mode of repression is mediated by direct interactions with *Hox* regulatory elements, independent of chromatin marks typically associated with repressed *Hox* genes.

Introduction

Hox transcription factors have conserved roles in shaping the body plans of animals and function as major determinants of morphological and cellular diversity along the rostrocaudal axis (McGinnis and Krumlauf, 1992). In the vertebrate hindbrain and spinal cord *Hox* genes are thought to be essential in defining the identity and synaptic specificity of neurons required for vital behaviors such as respiration and locomotion (Dasen and Jessell, 2009; Trainor and Krumlauf, 2000). An early step in the assembly of motor circuits is the

© 2010 Elsevier Inc. All rights reserved

correspondence: jeremy.dasen@nyumc.org.

⁶These authors contributed equally to this work.

Publisher's Disclaimer: This is a PDF file of an unedited manuscript that has been accepted for publication. As a service to our customers we are providing this early version of the manuscript. The manuscript will undergo copyediting, typesetting, and review of the resulting proof before it is published in its final citable form. Please note that during the production process errors may be discovered which could affect the content, and all legal disclaimers that apply to the journal pertain.

establishment of precise connections between motor neurons (MNs) and their peripheral targets, requiring the generation of hundreds of distinct subtypes. *Hox* genes are particularly important for the specification of MNs involved in limb coordination and differentiate these diverse populations from those necessary for other motor functions. While the regional specialization of MNs appears to be established through *Hox* combinatorials and additional lineage specific factors (Dalla Torre di Sanguinetto et al., 2008; Jessell, 2000; Shirasaki and Pfaff, 2002), the precise mechanisms by which *Hox*-dependent subtypes are generated within discrete areas of the spinal cord are not fully understood.

More than half of the 39 chromosomally clustered *Hox* genes are expressed by MNs (Dasen et al., 2005), yet little is known with respect to the mechanisms underlying one prominent feature of their patterns within the CNS – the restriction of a majority of *Hox* genes to limb levels. Early in development *Hox* expression is controlled by gradients of retinoic acid (RA), fibroblast growth factors (FGFs), and Wnts which determine the initial spatial profile of *Hox* transcription in neural progenitors along the rostrocaudal axis (Bel-Vialar et al., 2002; Liu et al., 2001; Nordstrom et al., 2006). In general, the induction of a *Hox* gene is linked to its position along the chromosome: genes located at the more 5' end of a cluster are expressed more posteriorly and are induced by progressively higher levels of FGF, and this action is opposed by paraxial mesoderm-derived RA which induces 3' genes (Bel-Vialar et al., 2002; Liu et al., 2001). The sequential activation of *Hox* genes by signaling gradients defines anterior expression limits (Bel-Vialar et al., 2002), and these boundaries are thought to be maintained by the actions of polycomb group (PcG) repressive complexes which restrict *Hox* expression through repressive chromatin modifications (Deschamps et al., 1999; Soshnikova and Duboule, 2009). At posterior regions many *Hox* genes are however initially coexpressed in neuronal progenitors (Bel-Vialar et al., 2002; Deschamps et al., 1999), and only as cells differentiate begin to display mutually exclusive domains of expression (Dasen et al., 2003). Defining the steps which link the early induction of *Hox* genes to their expression and function during MN differentiation is critical in elucidating how diverse subtypes are generated.

One mechanism thought to shape the final pattern of *Hox* expression in the CNS involves cross regulatory interactions between *Hox* proteins and *Hox* genes. In the developing hindbrain the restricted pattern of *Hox* expression within rhombomeres is regulated by autoregulatory and feed forward transcriptional cascades (Tumpel et al., 2009). In spinal MNs *Hox* expression appears to be defined through cross-repressive interactions occurring soon after MNs are born, presumably acting to prevent the generation of neurons with an ambiguous *Hox* code (Dasen et al., 2003; Dasen et al., 2005). However, several questions relating to the workings of the MN *Hox* network remain unresolved: 1) Do *Hox* repressive interactions function simply to sharpen molecular boundaries between neuronal subtypes? 2) Is the high density of *Hox* genes expressed at limb levels established through regulation of certain *Hox* genes en masse? 3) Are the repressive interactions mediated by direct binding of *Hox* proteins to *Hox* regulatory elements? 4) How would loss of a *Hox* repressor affect MN identity and patterns of connectivity? Addressing these issues has been challenging due to the redundancies between *Hox* genes and the inherent difficulty in identifying DNA target sites.

Progress towards understanding how *Hox* genes contribute to the diversification of neuronal subtypes has emerged through examination of the programs controlling two aspects of MN differentiation - the specification of columnar and pool subtypes. Distinct groups of *Hox* genes operate at each of these early phases of MN differentiation. The establishment of a MN columnar identity directs axons toward broad target fields including limb, axial, and body wall muscles as well as neurons in the sympathetic chain (Landmesser, 2001). At brachial and lumbar levels of the spinal cord, *Hox6* and *Hox10* proteins initiate the

molecular programs that specify the lateral motor column (LMC) fates and ensure that these subtypes are generated in registry with the position of their limb targets (Dasen et al., 2003; Shah et al., 2004; Tarchini et al., 2005; Wu et al., 2008). Within LMC neurons, the activities of nearly two dozen *Hox* genes are required to generate the ~50 motor pool subtypes targeting specific muscles in the limb (Dasen et al., 2005). In contrast to limb levels, intervening thoracic levels of the spinal cord contain relatively few Hox-dependent subtypes (Dasen et al., 2005), a possible reflection of the reduced number and variety of synaptic targets (Gutman et al., 1993; Prasad and Hollyday, 1991; Smith and Hollyday, 1983). Thoracic MNs express Hox9 proteins (Liu et al., 2001) and contain columns projecting towards hypaxial muscles and sympathetic chain ganglia, and these populations appear to be relatively homogeneous in molecular profile.

Further insight into the role of the Hox network in MN differentiation has emerged from the analysis of mice lacking the transcription factor FoxP1, a putative cofactor required for deployment of Hox programs in spinal MNs. Each Hox-dependent step of MN diversification relies on FoxP1 activity, as in its absence segmentally restricted columnar and pool subtypes fail to be specified, Hox controlled molecular programs are lost, and MNs revert to an ancestral state (Dasen et al., 2008; Rousso et al., 2008). As a consequence, the normal topographic relationship between MN position and peripheral connectivity is dissolved and limb-level motor axons appear to select their targets at random (Dasen et al., 2008). The columnar and pool specific patterns of Hox expression are unaffected by *Foxp1* mutation, indicating that Hox repressive activities are preserved. These observations suggest that FoxP1 functions within the context of a preexisting Hox code, established through cross-repressive interactions, and engages this network to selectively activate downstream columnar and pool specific programs.

Genetic evidence supporting a repression-based strategy in the control of Hox profiles in the CNS has been mostly indirect, due to the presumed functional compensation (Maconochie et al., 1996; McIntyre et al., 2007) amongst the large numbers of *Hox* genes expressed by MNs. Nevertheless, we initiated a systematic analysis of MN differentiation in *Hox* mutants, based on the assumption that removal of individual or multiple *Hox* genes would clarify their role in MN specification and allow a more definitive assessment of the significance of Hox cross-repressive interactions. We find that a single *Hox* gene, *Hoxc9*, is required for the generation of thoracic MN subtypes, is essential for organizing the MN topographic map, and acts as a key repressor of the forelimb-level *Hox* network. We provide evidence that *Hoxc9* represses anterior *Hox* genes through direct interactions at *Hox* loci, while more posterior *Hox* genes are silenced by a distinct mechanism. Our studies indicate that *Hoxc9* has a central role in patterning neuronal fates within the spinal cord through its activities as a global repressor of multiple *Hox* genes, and in generating a permissive zone for the *Hox* network to specify diverse subtypes.

Results

Loss of Thoracic Motor Neuron Columnar Subtypes in *Hoxc9* Mutants

To better understand how Hox repressor activities contribute to the diversification of motor neurons in mouse we initiated an analysis of the expression patterns and loss of function phenotypes for 10 of the *Hox4–9* paralogs (*Hoxc4*, *c5*, *c6*, *c8*, *c9*, *a5*, *a6*, *a7*, *a9*, *d9*) expressed at brachial and thoracic levels of the spinal cord. Because of the profound phenotype of *Hoxc9* mutants, and observed in an ENU-induced *Hoxc9* mutation (K. Liem et al., in preparation), we focus here on the roles of *Hox9* genes. Studies in chick implicate *Hox9* paralogs in controlling the molecular identity of columnar subtypes generated at thoracic levels (Dasen et al., 2003), in particular MNs that innervate sympathetic chain ganglia and occupy the preganglionic motor column (PGC). To determine whether *Hox9*

genes function in PGC specification, we analyzed the expression of each of the four *Hox9* genes finding that *Hoxa9*, *Hoxc9*, and *Hoxd9* are expressed in ventral spinal cord at embryonic day (e) 11.5, while *Hoxb9* was excluded from postmitotic MNs (Figure S1A). *Hoxa9* and *Hoxd9* were expressed by MNs extending from thoracic to upper lumbar regions while *Hoxc9* expression was largely restricted to thoracic levels (Figure S1A).

We next characterized the expression of molecular markers for early aspects of MN identity and columnar differentiation in *Hoxa9*, *Hoxd9*, and *Hoxc9* mutant mice, focusing on the impact of loss of *Hox9* activity on MN generation and PGC differentiation at e11.5. Features of MN class identity, such as expression of the homeodomain proteins *Isl1/2* and *Hb9* as well as the cholinergic marker *vesicular acetylcholine transferase (VAChT)* were not reduced in *Hoxa9* and *Hoxd9* mutants (Figure S1B and data not shown), while in *Hoxc9* mutants the number of thoracic MNs was increased by ~30% (Figure 1A–1D and 1G). We next examined the expression of two markers that distinguish PGC neurons from other thoracic MN subtypes - neuronal nitric oxide synthase (nNOS) and phospho(p)-Smad1/5/8. In *Hoxc9* mutants expression of nNOS and p-Smad1/5/8 were not detected at any age examined (e11.5 – e13.5) (Figure 1H–1K) while in *Hoxa9* and *Hoxd9* mutants expression of these genes were unaltered (Figure S1B).

We next assessed how the loss of *Hoxc9* affected the specification of two additional motor columns present at thoracic levels: hypaxial motor column (HMC) and median motor column (MMC) neurons. The HMC is selectively generated at thoracic levels, projects to intercostal and abdominal muscles and is characterized by coexpression of *Hb9* and *Isl1* and the ETS domain protein *Er81* (Cohen et al., 2005; Dasen et al., 2008). In *Hoxc9* mutants the number of *Hb9*⁺*Isl1*⁺ cells was significantly reduced and thoracic expression of *Er81* was not detected (Figure 1G and 1L–1O). Neurons in the MMC are a Hox-independent population present at all rostrocaudal levels of the spinal cord, project to axial muscles, and coexpress the LIM homeodomain factors *Lhx3* and *Hb9* (Arber et al., 1999; Tsuchida et al., 1994). In *Hoxc9* mutants the number of *Lhx3*⁺*Hb9*⁺ MNs was unchanged at all levels, indicating MMC identity is preserved (Figure 1E–1G). Together these observations indicate that *Hoxc9* activity is specifically required for the emergence of molecular features for two thoracic-specific motor columns (PGC and HMC) but is dispensable for early aspects of MN identity and specification of MMC neurons.

Thoracic Motor Neurons Acquire an LMC Identity in the Absence of *Hoxc9*

What are the fate(s) of thoracic MNs which have lost *Hoxc9*? *Hox9* genes have been implicated in restricting *Hox6* paralog gene expression to brachial levels and determining the domain in which forelimb-innervating lateral motor column (LMC) neurons are generated (Blackburn et al., 2009; Dasen et al., 2003). In *Hoxc9* mutants we detected ectopic expression of *Hoxc6* mRNA and protein throughout thoracic spinal cord extending to the boundary between caudal thoracic and rostral lumbar levels (Figure 1P–Q, 1X, S4I–S4J). We next examined whether, as a consequence of *Hoxc6* derepression, genes normally restricted to brachial LMC neurons are induced at thoracic levels. At limb levels LMC neurons are characterized by the expression of retinaldehyde dehydrogenase-2 (RALDH2) and high levels of *FoxP1* (Dasen et al., 2008; Sockanathan and Jessell, 1998). The normal brachial expression of LMC markers was unaffected by *Hoxc9* mutation (Figure S1C). In contrast, analysis of *Hoxc9* mutants revealed ectopic *RALDH2*⁺ and *FoxP1*^{high} MNs throughout the thoracic domain of *Hoxc6* expression (Figure 1R–1W, 1X, S2). At lumbar levels MNs did not ectopically express *Hoxc6* and the position of *Hox10*⁺ LMC neurons was preserved (Figure S1D and data not shown).

At limb levels, activation of *FoxP1* and *RALDH2* initiates a program of MN “divisional” specification, which controls the dorsoventral projection patterns of motor axons in the limb.

This program is characterized by the selective expression of homeodomain factors, where medial division LMC MNs express high levels of *Isl1* and lateral MNs high levels of *Hb9* and *Lhx1* (Kania and Jessell, 2003; Tsuchida et al., 1994). In *Hoxc9* mutants this divisional pattern of homeodomain expression and MN settling was present at thoracic levels (Figure 1M, S1E). In addition a pattern of *Epha4* guidance receptor expression similar to lateral LMC MNs was induced (Figure S1E). Thus, in the absence of *Hoxc9* two thoracic-specific columns are lost, *Hoxc6* is derepressed in all thoracic segments, and MNs acquire the columnar and divisional fates of forelimb-level LMC neurons. At a molecular level the spinal cord comprises two continuous columns of LMC and MMC neurons extending from cervical to lumbar levels (Figure 1Y).

Consequences of Columnar Transformation on Axonal Projection Patterns

To further examine the impact of switching the columnar identity of thoracic MNs we assessed potential axonal connectivity defects in *Hoxc9* mutants. We bred *Hoxc9* mice to a transgenic line (*Hb9::GFP* mice) in which all motor axons are labeled with GFP (Arber et al., 1999) and analyzed PGC, HMC, and MMC projection patterns. Three major projection pathways are followed by thoracic MNs, corresponding to the three prominent columnar subtypes: MMC neurons project dorsally to axial muscles, HMC ventrolaterally to body wall muscles, and PGC ventromedially to sympathetic chain ganglia. We observed a profound reduction in axonal projections towards the sympathetic chain in *Hoxc9*^{-/-}; *Hb9::GFP* mice, consistent with a loss of PGC fate (Figures 2C–2F and S3). In contrast, motor axon projections towards limb and axial muscles were normal in *Hoxc9* mutants indicating LMC and MMC trajectories are preserved (Figure 2A–2D). Thus *Hoxc9* is required for both the molecular identity and establishing the peripheral connectivity of PGC MNs.

Although molecular features of HMC identity were lost in *Hoxc9* mutants, motor axon projections toward hypaxial muscles were present, and there was a >2-fold increase in the overall thickness of the intercostal nerves (16.6 ± 0.1 μm in control versus 39.2 ± 0.7 μm in *Hoxc9* mutants at e13.5, n>10) (Figures 2G–2H). Because HMC and LMC neurons are similar in their initial pursuit of a distal and ventral trajectory, we hypothesized that in the absence of an appropriate peripheral target many of the aberrant LMC MNs projected like HMC neurons. To test this idea we injected rhodamine dextran (RhD) conjugates into the intercostal nerves of control and *Hoxc9*^{-/-} mice and assessed the identity of retrogradely labeled neurons. In wildtype mice all RhD labeled MNs lacked FoxP1 expression while in *Hoxc9* mutants labeled neurons expressed high levels of FoxP1 (Figure 2I–2J). None of the RhD-labeled neurons expressed the MMC marker *Lhx3* in *Hoxc9* mutants, consistent with the preservation of this columnar subtype (Figure 2K–2N). These observations indicate in the absence of *Hoxc9* MNs fail to project to the sympathetic chain, and the ectopic LMC neurons follow the route normally taken by HMC neurons (Figure 2E–2F).

Hoxc9 is Cell Autonomously Required for Thoracic Fates and Restricting LMC Identity

Because *Hoxc9* is broadly expressed at thoracic levels, including the mesoderm surrounding the neural tube (Figure S4W), and these peripheral tissues are known sources of patterning cues that control Hox profiles and MN fates (Bel-Vialar et al., 2002; Ensini et al., 1998; Liu et al., 2001), we performed experiments to determine whether *Hoxc9* is cell autonomously required for PGC and HMC specification and restriction of *Hoxc6*. To ablate *Hoxc9* expression selectively in spinal neurons we electroporated double stranded (ds) RNAs directed against *Hoxc9* into stage 14 chick neural tube and examined the effects on Hox expression and columnar fates after 2–3 days of further development. Coelectroporation of *Hoxc9* dsRNA with a nuclear LacZ expression plasmid (to mark electroporated cells) led to a significant reduction of *Hoxc9* protein in the spinal cord (Figure 3A–3B). Knockdown of

Hoxc9 had no effect on markers for early aspects of MN identity nor did it affect expression of Hoxa9, indicating the effect is specific for *Hoxc9* (Figure 3C and data not shown).

Consistent with the phenotype observed in mice lacking *Hoxc9*, after RNAi-mediated Hoxc9 ablation expression of Hoxc6 was detected in thoracic MNs (Figure 3G). Ectopic Hoxc6 expression was found only in neurons which had lost Hoxc9 indicating the effects are cell autonomous. In addition MNs that had lost Hoxc9 expressed LMC molecular determinants (RALDH2), failed to express markers for PGC MNs (pSmad), and there was a reduction of MNs with an HMC molecular profile (Figure 3D–3F). Thus Hoxc9 function is required within MNs for the generation of PGC and HMC neurons and the restriction of LMC fates. These observations suggest that thoracic MNs have the capacity to express Hoxc6 relatively late in development in the absence of changes in peripheral signals. In addition the RNAi experiments rule out the possibility that the alteration in Hoxc6 expression in *Hoxc9* mutants is due to changes in *cis*-regulatory elements within the *Hox-c* locus.

Hoxc9 as a Global Regulator of Anterior Hox Genes

Within the ~50 motor pools present in brachial LMC neurons the profiles of *Hox* gene expression are determined through cross-repressive interactions between multiple *Hox* genes expressed at specific rostrocaudal and intrasegmental levels (Dasen and Jessell, 2009). While the selectivity of these interactions has been studied in LMC neurons, the potential influences of Hox9 proteins on the forelimb Hox network have not been fully explored. In *Hoxc9* mutants and RNAi knockdown animals we found, unexpectedly, that all brachially-restricted *Hox* genes became derepressed at thoracic levels. A total of eight *Hox* genes, *Hoxa4*, *Hoxc4*, *Hoxa5*, *Hoxc5*, *Hoxa6*, *Hoxc6*, *Hoxa7*, and *Hoxc8* were ectopically expressed or markedly upregulated in thoracic MNs after Hoxc9 removal (Figure 3G–3V, S4I–S4N). *Hoxd9* was absent from MNs that expressed anterior *Hox* genes, while *Hoxa9* was retained, suggesting some but not all aspects of thoracic “Hox identity” are eroded (Figure 3W–3X, S4O–S4P). The alterations in Hox profiles also appeared to reflect a broad function of Hoxc9 since in *Hoxc9* mutants *Hox4–8* genes were derepressed throughout the ventral spinal cord as well as in the surrounding mesoderm (Figure S4Q–S4X). These observations indicate that Hoxc9 is required throughout the embryo for restricting expression of more anterior *Hox* genes.

Do the observed changes in Hox profiles reflect a specific Hoxc9 function or a more general hierarchical relationship of posterior over anterior *Hox* genes? To address this question we analyzed additional mutants for *Hox* derepression within the spinal cord. *Hoxa9* and *Hoxd9* mutants did not express *Hox4–8* genes at thoracic levels, consistent with the lack of changes in columnar fates (data not shown). We also analyzed *Hoxa7* and *Hoxc8* mutants, two genes expressed at brachial levels and at rostral thoracic regions. We did not observe a significant derepression of *Hox4*, *Hox5* or *Hox6* genes at thoracic levels in these mutants (data not shown). The brachial expression pattern of the more anterior *Hox* gene was similar to wildtype mice along the rostrocaudal axis in single mutants for *Hoxc5*, *Hoxc6*, *Hoxa6*, and *Hoxa7* analyzed at e11.5 (data not shown). We conclude that Hoxc9 has a selective role in confining *Hox4–Hox8* paralog expression to brachial levels (Figure 3Y).

Hoxc9 Expression is Sufficient to Suppress Limb-Level Hox Profiles and MN Fates

To further explore the repressive influences of Hoxc9, we examined the effects of misexpression in MNs. We used the regulatory sequences of the *Hb9* gene to target expression to postmitotic MNs, and performed founder analysis of *Hb9::Hoxc9* mice at e12.5 (Figure 4K–4L). Each of the *Hox* paralogs expressed by brachial MNs including Hoxc4, Hoxa5, Hoxc6, Hoxa7 and Hoxc8 were repressed or markedly downregulated in *Hb9::Hoxc9* mice, consistent with a broad repressive function of Hoxc9 (Figure 4A–4J).

Expression of *Hoxc9* did not affect expression of *Hoxa9* indicating the influences are specific for a subset of *Hox* genes (Figure S5E–S5F). The effects also proved to be cell autonomous, as *Hox* repression was restricted to MNs and appropriate *Hox* patterns were preserved in ventral interneurons (Figure 4A–4J). Thus *Hoxc9* is capable of regulating a subset of *Hox* genes through repressive functions in MNs.

Previous gain of function studies in chick indicate that *Hoxc9* activity prevents LMC specification by repressing *Hox6* genes, while its activities in MN progenitors are required for PGC specification (Dasen et al., 2003). Consistent with these observations, postmitotic *Hoxc9* expression under *Hb9* control was not sufficient to induce PGC fate, and MNs appeared to remain in an HMC-like ground state (Figures 4M–4N, S5A–S5D). In contrast when *Hoxc9* was activated in MN progenitors, by breeding mice containing a *pCAGGS-loxP-stop-loxP-Hoxc9* cassette to *Olig2::Cre* mice, ectopic PGC neurons were detected at brachial levels (Figure S5G–S5L). In *Hb9::Hoxc9* embryos expression of the LMC markers RALDH2 and FoxP1 were lost, and MNs also failed to express the pool marker *Pea3*, indicating that both *Hox*-dependent columnar and pool programs are blocked by *Hoxc9* (Figure 4O–4T). Thus the absence of *Hoxc9* expression from brachial levels appears necessary for MNs to express their appropriate *Hox* complement and execute their limb-level differentiation programs.

Assessment of the Functional Equivalence of *Hox9* Paralogs

The apparent unique role of *Hoxc9* in MN organization raises the question of whether the two other *Hox9* paralogs expressed by MNs, *Hoxa9* and *Hoxd9*, have a similar capacity to restrict expression of brachial *Hox* genes. We therefore examined *Hoxa9* and *Hoxd9* activities by misexpression in the chick neural tube. Previous studies have shown that *Hoxa9* can convert LMC MNs to PGC neurons (Dasen et al., 2003), although the influence of *Hoxa9* on brachial *Hox* expression was not assessed. We find that misexpression of *Hoxa9* at brachial levels can repress the same group of *Hox4–8* genes regulated by *Hoxc9* (Figure S5M–S5P). Because *Hoxa9* is still expressed in *Hoxc9* mutants (Figure S4O–S4P), the absence of functional compensation by *Hoxa9* is most likely a reflection of low levels of expression within the spinal cord.

Our gain of function analysis indicates that *Hoxd9* is functionally distinct from *Hoxa9* and *Hoxc9*. We find that brachial misexpression of *Hoxd9* fails to induce PGC neurons, nor does it inhibit LMC specification (Figure S5Q–S5S). We unexpectedly find that elevating the levels of *Hoxd9* at thoracic levels can induce LMC fates (Figure S5T). As with *Hoxa9* and *Hoxc9* misexpression, anterior *Hox* genes were repressed after brachial *Hoxd9* misexpression suggesting *Hoxd9* functions by promoting lumbar over brachial LMC identity (Figure S5U–S5X). In *Hoxc9* mutants *Hoxd9* expression is lost by MNs (Figure 3W–3X), thereby negating any potential repressive influence of *Hoxd9* on the derepressed *Hox* genes. Taken with the observation that in *Hoxa9* and *Hoxd9* mutants anterior *Hox* genes are not derepressed, these data support the notion that *Hoxc9* alone has a central role in restricting *Hox4–8* gene expression from thoracic levels.

Thoracic *Hox* Derepression Alters Motor Pool Organization

The combinatorial actions of *Hox4–8* genes are critical in the specification of motor pools targeting the forelimb. The expansion of all brachial *Hox* genes into thoracic levels raises the question of whether the network specifying pools might be preserved in a limbless environment and would generate the appropriate fates for a given transcriptional code. In principle *Hox* derepression could lead to several outcomes including 1) a scrambling of *Hox* codes for pool fates, 2) a wholesale shift of pools into the thoracic domain, or 3) the overall expansion of pools from brachial to thoracic levels. We assessed these possibilities by

analyzing the expression and connectivity patterns of MNs expressing the transcription factors *Pea3* and *Scip*, which mark pools within caudal LMC regions.

Expansion of the *Pea3* motor pool in *Hoxc9* mutants—*Pea3* expression is initially controlled by a network involving *Hox4*, *Hoxc6*, and *Hoxc8* activities and marks MNs targeting the cutaneous maximus (CM) muscle (Figure 5A) (Livet et al., 2002). While the normal domain of *Pea3* was grossly unaltered in *Hoxc9* mutants, *Pea3* expression was expanded throughout thoracic levels (Figure 5B–5C, 5R, S6A–S6D). Ectopic *Pea3* MNs expressed *Hoxc6* and *Hoxc8*, two proteins implicated in control of *Pea3* expression (Figure S6A–S6H). Downstream targets of *Pea3*, including *Cadherin8* and *Sema3E*, as well as *Cadherin20* (Livet et al., 2002) were detected at thoracic levels in *Hoxc9* mutants (Figure 5D–5I). Analysis of *Hoxc9* RNAi knockdown animals also revealed ectopic *Pea3* neurons at thoracic levels (Figure 5W and S6R). These observations indicate that the network controlling *Pea3* can operate in the thoracic environment.

We next assessed whether the presence of ectopic *Pea3*⁺ MNs in *Hoxc9* mutants causes a redirection of motor axons to the CM. We first assessed projections to the CM using whole mount immunohistochemistry, finding that the level of innervation was similar between wildtype and mutant animals (Figure 6A–6B, S7G–S7J). We then performed retrograde tracing assays to ascertain the behavior of the ectopic populations of *Pea3* MNs. Injection of RhD into the CM nerve labeled *Pea3*⁺ MNs that were confined to the normal brachial domain in *Hoxc9* mutants (Figure 6E–6I). Injection into intercostal nerves revealed that the ectopic *Pea3* MNs projected along the pathway normally followed by HMC neurons (Figure 6J–6L). This result was unexpected, as *Pea3* expression relies on glial-derived neurotrophic factor (GDNF) signaling from the limb (Haase et al., 2002). Analysis of *GDNF* expression however revealed that in addition to the CM the intercostal mesoderm is a source of GDNF thus providing a permissive context for *Pea3* induction (Figure S7A–S7F). In *Hoxc9* mutants there is therefore an overall expansion of the *Pea3* motor pool with the majority of ectopic MNs targeting inappropriate muscles.

Altered pool position and connectivity of *Scip* MNs in *Hoxc9* mutants—We next analyzed the expression of the pool marker *Scip* which marks MNs projecting along the ulnar and median nerves (Dasen et al., 2005). *Scip* expression is confined to the most caudal brachial LMC MNs and is controlled by a network requiring *Hoxc8*, and the late exclusion of *Hoxc6* (Figure 5A) (Dasen et al., 2005). We have additionally found that *Scip*⁺ MNs express low levels of *Hoxc9* (Figure S6O–S6Q), suggesting a possible role in *Hoxc6* restriction. Consistent with this idea we observed an upregulation of *Hoxc6* at caudal brachial levels in *Hoxc9* mutants and the number of *Scip*⁺ MNs was reduced (Figure 5J–5M). The loss of *Scip* MNs was associated with a reciprocal increase in the number of brachial *Pea3*⁺ MNs (Figure 5R) consistent with the idea that this pool is specified by a *Hoxc6* + *Hoxc8* code. *Scip*⁺ MNs were detected in *Hoxc9* mutants, although this population was shifted to thoracic spinal cord (Figure 5N–5Q, 5R and S6S–S6T), where *Hoxc6* levels are apparently reduced in a subset of MNs at the time of pool specification (Figure 5Q).

How does the altered position of *Scip* MNs affect the pattern of limb innervation? At e12.5 projections along the ulnar and medial nerves were consistently stunted in *Hoxc9* mutants (Figure 6A–6B). By e13.5 there was a loss in the distal arbors of the median nerve and the density of ulnar projections was reduced (Figure 6C–6D). We then performed tracing assays to assess the identity of the few neurons projecting into the ulnar nerve and to define the target of ectopic *Scip* MNs. Ulnar injections of RhD in wildtype mice labeled clusters of LMC neurons that expressed *Scip*, while injections in *Hoxc9* mutants labeled fewer neurons which were scattered and lacked *Scip* expression (Figure 6O–6Q). Retrograde tracing indicated that, like the ectopic *Pea3*⁺ MNs, the aberrant *Scip*⁺ neurons project along

intercostal nerves (Figure 6M–6N and 6R–6S). Thus in the absence of *Hoxc9* there is an erosion of the normal topographic relationship between the identity and projection pattern of motor pools, with the most dramatic effects on the innervation of distal limb muscles.

Characterization of the behavior of ectopic motor pools in *Hoxc9* mutants—

Additional aspects of the programs controlling MN pool fates were deployed at thoracic levels in *Hoxc9* mutants. *Pea3* and *Scip* MNs normally settle in distinct positions, with the *Scip* pool positioned dorsal to the *Pea3* pool. This migratory behavior was retained in the thoracic environment and the ectopic *Scip*⁺ and *Pea3*⁺ MNs were well clustered (Figure 5S–5T). The specification of these pools requires exclusion of the transcription factor *Meis1* (Dasen et al., 2005) and this Hox-dependent program was recapitulated at thoracic levels (Figure 5U–5V). The appearance of ectopic *Pea3* and *Scip* MNs was also dependent on “motor pool” *Hox* genes, since dual RNAi-mediated knockdown of *Hoxc9* and *Hoxc8* in chick failed to generate ectopic *Pea3* or *Scip* MNs, although ectopic LMC neurons were still present (Figure 5X–5Y, S6U–S6V). Together these observations indicate that under conditions of Hox derepression, this network is capable of specifying multiple facets of pool identity.

We next considered the possibility that the ectopic LMC pools in *Hoxc9* mutants target specific groups of hypaxial muscles. Although the muscle-specific branches of intercostal nerves are too small to inject with tracers individually, we were able to inject at the initial bifurcation that segregates “internal” from “external” HMC axons. Interestingly, we find that injection of internal intercostal nerves in *Hoxc9* mutants labeled LMC-like MNs that express *Isl1* and lacked *Lhx1* (Figure S7K–S7N). In addition all ectopic *Scip* neurons expressed *Isl1*, lacked *Lhx1*, and were labeled after internal intercostal nerve injections (Figure S7O–S7R). These observations suggest the ectopic LMC MNs do not project randomly into hypaxial muscle but may target specific muscle groups.

***Hoxc9* Binds Multiple Regions within the *Hox-a* and *Hox-c* Clusters**

The derepression of a battery of *Hox* genes in *Hoxc9* mutants suggests that the entire set is controlled in a concerted manner. Derepression could be a consequence of *Hoxc9* acting on multiple *Hox* genes or could be a result of derepression of a Hox protein that coordinates brachial *Hox* gene activation. To determine whether *Hoxc9* binds directly to *Hox* regulatory elements, we used an unbiased approach by taking advantage of an embryonic stem (ES) cell differentiation protocol that recapitulates MN development and allows generation of large quantities of material conducive for biochemical studies (Wichterle et al., 2002). To activate *Hoxc9* expression during MN differentiation, epitope (V5) -tagged *Hoxc9* was induced as cells become MN progenitors and was maintained until the end of differentiation. We first validated this approach by analyzing the effect of *Hoxc9* expression on Hox profiles in ES cell derived MNs which, under standard conditions, are programmed to a rostral cervical (i.e. *Hox4*⁺ and *Hox5*⁺) identity. Similar to *in vivo* observations, *Hoxc9* induction repressed rostral *Hox* genes including *Hoxc4* and *Hoxa5* (Figure 7A–B). Thus *Hoxc9* retains its normal repressor function in the context of ES-cell derived MNs.

We next performed chromatin immunoprecipitation assays followed by sequencing of the enriched DNA fragments (ChIP-seq) to identify potential binding regions within the *Hox-c* and *Hox-a* loci. The most over-represented binding motif at enriched sites was similar to the site described for *Hox9* paralogs obtained from *in vitro* studies (Shen et al., 1997) suggesting that tagged *Hoxc9* binds to cognate sequences (Figure 7C). Analysis of the location of binding regions indicated that *Hoxc9* associates with genomic regions located 3' to the position of *Hox9* genes (Figure 7C), including genes derepressed in *Hoxc9* mutants. It is of note that the *Hox4–6* paralogs, which display mutually exclusive patterns of expression with *Hoxc9*, contain binding sites situated within the first intron. In contrast both *Hoxa7* and

Hoxc8, whose expression overlaps with *Hoxc9* at rostral thoracic levels, do not contain an intronic binding site, but rather a potential site located more distally (Figure 7C). Certain *Hox* genes may therefore have evolved differential sensitivities to *Hoxc9* repression, with the regulatory sequences retaining conserved positions within *Hox* loci.

Genome-wide analysis of *Hoxc9* binding sites was performed in the context of ES-derived cervical MNs, raising the question of whether a similar occupancy is present at thoracic levels *in vivo*. We therefore performed ChIP assays on chromatin prepared from e12.5 thoracic spinal cord. We took advantage of the observation that most thoracic spinal neurons, including MNs and interneurons, express *Hoxc9* protein and provide a relatively pure population for ChIP analysis (Figure 1A). We found that the majority of the regions identified by ChIP-seq were coimmunoprecipitated with a *Hoxc9* antibody when compared to control IgG (Figure 7D). In both assays *Hoxc9* was not associated with its own promoter, nor was *Hoxc9* associated with the promoter regions of *Hoxc10* or *Hoxd10* (Figure 7C–7D) in agreement with the finding that these genes are not derepressed in *Hoxc9* mutants. These observations additionally suggest a distinct transcriptional mechanism to exclude lumbar *Hox10* genes from thoracic spinal cord.

Studies in several systems indicate that *Hox* gene expression is regulated in part through chromatin modifications at specific lysine residues on histone H3. The repressed state of *Hox* genes are initiated and maintained by the actions of the polycomb group (PcG) complexes which promote the trimethylation of histone H3 at lysine 27, and subsequent interactions with associated repressor proteins (Schuettengruber and Cavalli, 2009). Using ChIP assays we assessed whether this repressive mark (H3K27me3) is present on brachial *Hox* genes at thoracic levels. Remarkably, none of the anterior *Hox* genes which were derepressed in *Hoxc9* mutants were associated with high levels of the H3K27me3 mark (Figure 7E). In contrast more posteriorly expressed *Hox* genes, including *Hoxc10* and *Hoxd10* were trimethylated at K27 on H3 at thoracic levels (Figure 7E). When H3K27me3 ChIP was performed at brachial levels we found that both *Hoxc9* and *Hox10* promoters were associated with this repressive mark, suggesting that the exclusion of *Hoxc9* from brachial MNs involves histone methylation-dependent silencing (Figure 7F). These observations indicate that different levels of the spinal cord exclude *Hox* genes by distinct mechanisms and are likely to explain why anterior *Hox* genes are derepressed at thoracic levels in *Hoxc9* mutants while more posterior *Hox* genes retain their normal expression patterns.

Discussion

Hox genes are essential in the specification of vertebrate CNS cell types, although the strategies used to achieve specific *Hox* patterns during neuronal differentiation are poorly understood. We have found that a critical step in the transition from the early induction of *Hox* gene expression to the regionally restricted patterns in MNs is mediated through the actions of a broadly acting *Hox* gene repressor. These findings may have more general implications for understanding how *Hox* networks contribute to the diversification of other vertebrate cell types.

Our studies are consistent with the idea that MN diversity is established through a repression-based network, with *Hoxc9* functioning as a selective determinant of thoracic columnar fates. In the absence of *Hoxc9*, motor columns typically associated with respiratory (HMC neurons) and autonomic (PGC) neuronal networks are lost and body wall muscles are appropriated by motor neurons that have acquired the molecular identity of cells involved in limb control. An unexpected finding in our analysis is that *Hoxc9* has an additional role in shaping the overall organization of the motor system, by acting as a global repressor of anterior *Hox* genes and confining the diversity of MN subtypes to limb levels.

Genome-wide analysis of *Hoxc9* binding suggests that *Hox* gene repression is mediated through interactions at several loci within the *Hox-a* and *Hox-c* clusters. Furthermore, analysis of MN pool disorganization in *Hoxc9* mutants provides insights into the strategies used to generate diverse subtypes. We discuss these findings in the context of *Hox* transcriptional networks and the control of CNS cell type diversification.

A Unique Role for *Hoxc9* in Motor Neuron Columnar Fate Specification

While studies in invertebrate systems have established that *Hox* genes are crucial in the organization of body plans (McGinnis and Krumlauf, 1992), progress towards addressing *Hox* function in the vertebrate CNS has been thwarted by functional redundancies amongst paralog groups. In a systematic analysis of MN defects in *Hox* mutants we found that mutation of a single gene, *Hoxc9*, leads to a remarkably pervasive and fully penetrant phenotype. *Hoxc9* mutants lack PGC and HMC neurons with the consequence that all thoracic MNs are transformed into an LMC molecular identity (Figure 8A). This specific activity contrasts with limb levels of the spinal cord, where several *Hox* genes appear to be necessary to establish the LMC columnar fate. At least three *Hox* genes, *Hoxa10*, *Hoxc10* and *Hoxd10* are required for establishing hindlimb LMC identity (Rousso et al., 2008; Tarchini et al., 2005; Wu et al., 2008) while forelimb LMC specification requires multiple *Hox* paralogs including *Hox6* and *Hox8* genes (Dasen et al., 2003; Vermot et al., 2005). In addition the lack of any discernable columnar phenotype in single mutants for *Hoxa5*, *Hoxa6*, *Hoxa7*, *Hoxa9*, *Hoxc4*, *Hoxc5*, *Hoxc6*, *Hoxc8*, and *Hoxd9* indicates that *Hoxc9* has a unique function in shaping the early organization of spinal motor columns.

In conjunction with previous observations, our findings suggest that *Hoxc9* controls the identity of thoracic motor columns through distinct repressive and activator functions. When *Hoxc9* is misexpressed in brachial progenitors, presumptive LMC MNs are programmed to a PGC identity, indicating that *Hoxc9* has an active role in promoting PGC fate. PGC neurons additionally require specific *Hoxc9* activator function, since dominant repressor derivatives fail to respecify LMC MNs, although *Hox* cross-repressive activities are retained (Dasen et al., 2003). The ability of *Hoxc9* to promote PGC fates is likely to be dependent on interactions with the accessory factor *FoxP1*, since *FoxP1* is also required for the specification of PGC MNs (Dasen et al., 2008; Rousso et al., 2008). *Hoxc9*/*FoxP1* interactions may therefore facilitate activities at target genes that are distinct from the sites repressed by *Hoxc9* described in this study.

In contrast the switch of HMC neurons to an LMC fate in *Hoxc9* mutants can be attributed to the loss of *Hoxc9* repressor function. HMC neurons are normally specified in a *Hox*-independent manner, as in mice lacking *Foxp1* both PGC and LMC MNs are switched to an HMC fate, independent of position or *Hox* profile (Dasen et al., 2008; Rousso et al., 2008). These observations suggest that the transformation of HMC to LMC MNs in *Hoxc9* mutants is due to the derepression of LMC-promoting *Hox* genes, while the loss of PGC neurons reflects a requirement for *Hox* activator function. More generally the phenotype of *Hoxc9* mutants fits well with a dual functionality for *Hox* proteins in cell type specification (Li and McGinnis, 1999), through their ability to both activate differentiation programs as well as restrict expression of determinants of other subtypes, even within the same cell.

Strategies for Coordinating Neuronal Diversity with the Periphery

Given the redundancies amongst vertebrates *Hox* genes why would a single thoracic *Hox* gene exert a central role in MN organization? Vertebrate species vary widely in the number of thoracic segments, ranging from as few as 6 in frogs to over 300 in certain species of snakes (Dequeant and Pourquie, 2008), and these morphological differences are thought to be shaped by regional *Hox* gene activities (Wellik, 2009). One possibility is that *Hoxc9* is

similar to *DrosophilaHox* genes, by acting as a global determinant of thoracic identity. *Hoxc9* function in MNs however does not appear to be associated with the patterning of the thoracic skeletal structures, since these programs are grossly preserved in *Hoxc9* mutants (McIntyre et al., 2007). Previous studies have implicated multiple *Hox9* paralogs in specifying the regional identity of the lateral plate mesoderm that determines the rostrocaudal position where thoracic segments and limbs form (Cohn et al., 1997). Since *Hoxc9* defines the identity of MNs that project into thoracic segments, as well as the position in which limb-innervating MNs are generated, one possibility is that the utilization of a single *Hox* gene for this purpose allows for a certain degree of adaptability specifically within the motor system, with additional *Hox9* genes functioning to coordinately pattern mesoderm-derived structures.

Despite the lack of global morphological changes in *Hoxc9* mutants we find that in addition to MNs several *Hox* genes are derepressed within thoracic mesoderm. Although the significance of this observation is unclear, several studies implicate *Hox* genes in specifying the precursors that give rise to MN target tissues. In the somites *Hox* genes have been shown to control the migratory behavior of myogenic precursors that generate the limb musculature (Alvares et al., 2003) while in the limb mesenchyme *Hox* genes have been implicated in the spatial organization of axonal guidance cues (Burke and Tabin, 1996). These *Hox* dependent steps in patterning mesodermal derivatives may serve to coordinate the specification of MN subtypes with peripheral signals that help shape motor axon target selection. Thus an additional role of *Hoxc9* may be to pattern target regions, by restricting expression of certain *Hox* genes to forelimb level somitic and lateral plate mesoderm.

Hox Cross-Repression and the Emergence of MN Topographic Maps

Our studies indicate that *Hoxc9* acts at an early stage of MN differentiation, by partitioning thoracic and limb-level subtypes, and through restricting *Hox4–8* gene expression to brachial LMC MNs. This group of *Hox* genes has been shown to function as a network to specify the fates of the ~50 motor pools innervating the forelimb (Dasen et al., 2005). We find in *Hoxc9* mutants that several downstream aspects of the motor pool *Hox* network are deployed in thoracic spinal cord, characterized by an expansion of pools expressing *Pea3* and *Scip*, the induction of pool migratory behaviors, and expression of synaptic specificity determinants. As a consequence of *Hox* derepression there is a loss in the normal topographic relationship between MN position and peripheral target specificity, as most of the ectopic subtypes target inappropriate muscles. Nevertheless these findings are in agreement with a model in which early aspects of the programming of MNs identities, including their columnar, divisional, and pool fates, emerge through a cell intrinsic network, independent of specific signals provided by the limb mesoderm or differentiated muscle.

Analysis of the specification of the motor pool expressing *Scip* provides additional clues into how the *Hox* network controls MN diversification. In *Hoxc9* mutants we observe a shift of the brachial *Scip* pool from its normal position, and an erosion of motor axon projections to the distal limb. Two observations suggest the identity of *Scip*⁺ MNs requires graded *Hoxc9* activity, as opposed to an absolute repressive function used to establish a sharp molecular boundary. In gain and loss of function assays *Hoxc9* exhibits repressive activities towards *Hoxc8* and *Hoxc6*, yet *Scip* neurons express low *Hoxc9* levels, retain *Hoxc8*, and lack *Hoxc6*. In addition at rostral thoracic levels many MNs coexpress *Hoxc9* and *Hoxc8* (Liu et al., 2001). These observations indicate that *Hoxc9* does not function through a “winner take all” style of cross-repression as occurs during the specification of progenitors along the dorsoventral axis (Briscoe and Ericson, 2001). Similar graded interactions amongst *Hox4–8* genes could be involved in the diversification of the ~50 pool fates within the LMC. More generally this strategy for the diversification of MN subtypes could apply to other CNS cell types programmed through networks of transcriptional repressors.

Transcriptional Mechanisms Controlling Hox Patterns in the CNS

Our studies provide insight into the mechanisms through which *Hox* gene expression boundaries are established during the specification of CNS cell types. The transcriptionally silenced state of *Hox* genes are maintained in part through the actions of PcG complexes, leading to the trimethylation of histone H3K27 and binding of additional factors which restrict promoter access to activating transcriptional machinery (Schuettengruber and Cavalli, 2009). CHIP analysis of thoracic spinal cord indicates that this mode of Hox repression is not used to silence brachial *Hox* genes, but rather is mediated through the actions of a single Hox factor. The idea that Hoxc9 directly represses *Hox* genes is supported by three lines of evidence: 1) Hoxc9 occupies a number of sites in the proximity of repressed *Hox* genes, 2) loss of Hoxc9 leads to ectopic expression of these same *Hox* genes at thoracic levels, and 3) misexpression of Hoxc9 represses brachial *Hox* genes. While *Hox* genes are known to be negatively regulated by micro- and long noncoding-RNAs (Rinn et al., 2007; Ronshaugen et al., 2005), it is unlikely that Hoxc9 acts through the induction of these regulatory molecules, since dominant-repressor Hoxc9 derivatives display similar repressive activities (Dasen et al., 2003). Although the precise mechanism by which Hoxc9 represses is unresolved, it may include more typical forms of gene regulation, such as selective recruitment of corepressors to be identified.

Hoxc9 mutation does not appreciably affect expression of more posterior lumbar-level *Hox* genes, raising the question of how they are spatially regulated. Our CHIP analysis of H3K27me3 patterns suggests a distinct mechanism for the restriction of more posterior *Hox* genes in the spinal cord. We find that at thoracic levels *Hox10* promoters contain the H3K27me3 repressive mark, and at brachial levels both *Hoxc9* and *Hox10* genes are characterized by the presence of this histone modification. The exclusion of more posterior *Hox* genes in MNs could therefore be mediated by the maintenance of repressive chromatin structure within a *Hox* cluster. Consistent with this idea, mice bearing mutations in PcG components are characterized by anterior shifts in *Hox* gene expression, whereas posterior boundaries are maintained (van der Lugt et al., 1996). Thus the mechanisms controlling Hox exclusion at a given segmental level appear to be directionally distinct: recruitment of a Hox protein for repression of anterior *Hox* genes and silencing of more posterior *Hox* genes through the actions of PcG complexes (Figure 8B).

Hox Repression in the Assembly of Spinal Neuronal Networks

While our studies have focused on repressive interactions during MN development, it is likely that *Hoxc9* and *Hox* genes in general play a broader role in shaping connections within motor networks. In addition to MNs, *Hoxc9* mutation causes a derepression of *Hox* genes in other cell types, including ventral interneurons. While the role of *Hox* genes in these diverse classes is unresolved, the local circuits of neurons which coordinate the rhythmic firing patterns of MNs during respiration and locomotion are known to occupy distinct rostrocaudal levels of the spinal cord (Ballion et al., 2001; Kjaerulff and Kiehn, 1996). It is possible that the shared expression of *Hox* genes in multiple neuronal classes helps establish selective connections in developing motor circuits. Hoxc9 may therefore have a more general role in specifying the regionally restricted subtypes essential for the emergence of motor behaviors through global regulation of neuronal *Hox* patterns.

Experimental Procedures

Mouse Genetics

The *Hox* mutant strains are described in McIntyre et al. (2007), the *Hb9::GFP* line in Arber et al., (1999). The *Hb9::Hoxc9* construct was generated as described (Dasen et al., 2003) and microinjected into mouse zygotes by standard procedures.

In Ovo Chick Electroporations

Electroporation was performed in chick embryos as described (Dasen et al., 2003). RNA interference was performed using 21-nucleotide dsRNAs (Dharmacon, Option A4). To identify electroporated neurons, siRNAs (suspended in TE to a final concentration 5mg/ml) were combined with a nuclear LacZ expression plasmid (0.5 mg/ml). Target sequence against chick *Hoxc9* was: 5'-CGAAGTAGCCCGAGTCCTA-3'. Results for each experiment are representative of at least eight electroporated embryos from three or more independent experiments in which the electroporation efficiency in MNs was >60%.

Chromatin Immunoprecipitation (ChIP) Assays

Brachial and thoracic spinal cords were dissected from e13.5 mouse embryos. Tissues were homogenized in 1.1% formaldehyde using a Dounce B homogenizer. Chromatin was extracted and fragmented to 500–1000 bp by sonication (12 pulses of 10 seconds at 50% amplitude with 50 seconds between pulses). Chromatin extracts (~20 ug) were incubated overnight at 4°C with either specific antibodies or species-matched IgGs. Antibodies used are: rabbit anti-*Hoxc9*, rabbit anti-H3K27me3 (Upstate). Protein A-agarose (Roche) was added for 3 hours at 4°C and the antibody-protein-DNA complexes were washed 7 times with RIPA and eluted in 1% SDS. DNA-protein decrosslinking was performed overnight at 65°C followed by RNase and proteinase K treatment at 55°C for 3 hours. DNA was purified using QIAquick columns (Qiagen). *Hox* regions were amplified using Power Sybr® Green PCR Master Mix (Applied Biosystems) and detected with Mx 3005P real-time PCR apparatus (Stratagene). Fold enrichment were calculated over IgG using the $\Delta\Delta C_t$ method: Fold enrichment = $2^{-(\Delta\Delta C_t)}$, where $\Delta\Delta C_t = (C_{tIP} - C_{tInput})_{thoracic} - (C_{tIgG} - C_{tInput})_{brachial}$. Primer sequences and details of the Chip-Seq are available in Supplemental Information.

In Situ Hybridization and Immunohistochemistry

In situ hybridization and immunohistochemistry were performed on 16 μ m cryostat sections as described (Tsuchida et al., 1994). Whole-mount GFP staining was performed as described (De Marco Garcia et al., 2008) and motor axons were visualized in projections of confocal Z-stacks (500–1000 μ m). Antibodies were generated as described (Dasen et al., 2008; Dasen et al., 2005; Liu et al., 2001; Tsuchida et al., 1994). Other antibodies were obtained and used as follows: rabbit anti-nNOS 1:5000 (Cryostar), goat anti-*Hoxc6* 1:2000 (Santa Cruz), rabbit anti-GFP 1:1000 (Invitrogen). A *Hoxc9* antibody was generated in guinea pigs using the peptide sequence: DSLISHENEELLASRFPTKKC.

Retrograde Labeling of Motor Neurons

Retrograde labeling of MNs was performed as described (Dasen et al., 2008). Lysine-fixable dextran-tetramethylrhodamine (RhD, Molecular Probes) was injected into severed muscle-specific nerves of e12.5–e13.5 embryos. To aid in the identification of nerves, we used GFP fluorescence from *Hb9::GFP* transgenic mouse embryos, visualized using a MVX10 wide-field fluorescent microscope (Olympus). Nerves were severed using Oban Bioscissors and RhD was injected onto the cut terminal. Embryos were incubated for 4 to 5 hours in oxygenated F12/DMEM (50:50) solution at 32–34°C and subsequently fixed in 4% paraformaldehyde.

Supplementary Material

Refer to Web version on PubMed Central for supplementary material.

Acknowledgments

We thank Tom Jessell, Gord Fishell and members of the lab for comments on the manuscript. Mario Capecchi and Deneen Wellik provided *Hox* mutant lines, Tom Jessell provided *Olig2::Cre mice*, and Silvia Arber provided Pea3 antibodies. We thank NYU transgenic facility for mouse husbandry, and Brian Dynlacht for help with the in vivo ChIP assays. EOM is supported by Damon Runyon Cancer Research Foundation. JD is supported by grants from the Alfred P. Sloan Foundation, Burroughs Wellcome Fund, McKnight Foundation, NIH R01 NS062822 and Project ALS. JD is an HHMI Early Career Scientist.

References

- Alvares LE, Schubert FR, Thorpe C, Mootoosamy RC, Cheng L, Parkyn G, Lumsden A, Dietrich S. Intrinsic, Hox-dependent cues determine the fate of skeletal muscle precursors. *Dev Cell* 2003;5:379–390. [PubMed: 12967558]
- Arber S, Han B, Mendelsohn M, Smith M, Jessell TM, Sockanathan S. Requirement for the homeobox gene Hb9 in the consolidation of motor neuron identity. *Neuron* 1999;23:659–674. [PubMed: 10482234]
- Ballion B, Morin D, Viala D. Forelimb locomotor generators and quadrupedal locomotion in the neonatal rat. *Eur J Neurosci* 2001;14:1727–1738. [PubMed: 11860467]
- Bel-Vialar S, Itasaki N, Krumlauf R. Initiating Hox gene expression: in the early chick neural tube differential sensitivity to FGF and RA signaling subdivides the HoxB genes in two distinct groups. *Development* 2002;129:5103–5115. [PubMed: 12399303]
- Blackburn J, Rich M, Ghitani N, Liu JP. Generation of conditional Hoxc8 loss-of-function and Hoxc8->Hoxc9 replacement alleles in mice. *Genesis* 2009;47:680–687. [PubMed: 19621436]
- Briscoe J, Ericson J. Specification of neuronal fates in the ventral neural tube. *Curr Opin Neurobiol* 2001;11:43–49. [PubMed: 11179871]
- Burke AC, Tabin CJ. Virally mediated misexpression of Hoxc-6 in the cervical mesoderm results in spinal nerve truncations. *Dev Biol* 1996;178:192–197. [PubMed: 8812121]
- Cohen S, Funkelstein L, Livet J, Rougon G, Henderson CE, Castellani V, Mann F. A semaphorin code defines subpopulations of spinal motor neurons during mouse development. *Eur J Neurosci* 2005;21:1767–1776. [PubMed: 15869472]
- Cohn MJ, Patel K, Krumlauf R, Wilkinson DG, Clarke JD, Tickle C. Hox9 genes and vertebrate limb specification. *Nature* 1997;387:97–101. [PubMed: 9139829]
- Dalla Torre di Sanguinetto SA, Dasen JS, Arber S. Transcriptional mechanisms controlling motor neuron diversity and connectivity. *Curr Opin Neurobiol* 2008;18:36–43. [PubMed: 18524570]
- Dasen JS, De Camilli A, Wang B, Tucker PW, Jessell TM. Hox repertoires for motor neuron diversity and connectivity gated by a single accessory factor, FoxP1. *Cell* 2008;134:304–316. [PubMed: 18662545]
- Dasen JS, Jessell TM. Hox networks and the origins of motor neuron diversity. *Curr Top Dev Biol* 2009;88:169–200. [PubMed: 19651305]
- Dasen JS, Liu JP, Jessell TM. Motor neuron columnar fate imposed by sequential phases of Hox-c activity. *Nature* 2003;425:926–933. [PubMed: 14586461]
- Dasen JS, Tice BC, Brenner-Morton S, Jessell TM. A Hox regulatory network establishes motor neuron pool identity and target-muscle connectivity. *Cell* 2005;123:477–491. [PubMed: 16269338]
- Dequeant ML, Pourquie O. Segmental patterning of the vertebrate embryonic axis. *Nat Rev Genet* 2008;9:370–382. [PubMed: 18414404]
- Deschamps J, van den Akker E, Forlani S, De Graaff W, Oosterveen T, Roelen B, Roelfsema J. Initiation, establishment and maintenance of Hox gene expression patterns in the mouse. *Int J Dev Biol* 1999;43:635–650. [PubMed: 10668974]
- Ensini M, Tsuchida TN, Belting HG, Jessell TM. The control of rostrocaudal pattern in the developing spinal cord: specification of motor neuron subtype identity is initiated by signals from paraxial mesoderm. *Development* 1998;125:969–982. [PubMed: 9463344]
- Gutman CR, Ajmera MK, Hollyday M. Organization of motor pools supplying axial muscles in the chicken. *Brain Res* 1993;609:129–136. [PubMed: 8508296]

- Haase G, Dessaud E, Garces A, de Bovis B, Birling M, Filippi P, Schmalbruch H, Arber S, deLapeyriere O. GDNF acts through PEA3 to regulate cell body positioning and muscle innervation of specific motor neuron pools. *Neuron* 2002;35:893–905. [PubMed: 12372284]
- Jessell TM. Neuronal specification in the spinal cord: inductive signals and transcriptional codes. *Nat Rev Genet* 2000;1:20–29. [PubMed: 11262869]
- Kania A, Jessell TM. Topographic motor projections in the limb imposed by LIM homeodomain protein regulation of ephrin-A:EphA interactions. *Neuron* 2003;38:581–596. [PubMed: 12765610]
- Kjaerulff O, Kiehn O. Distribution of networks generating and coordinating locomotor activity in the neonatal rat spinal cord in vitro: a lesion study. *J Neurosci* 1996;16:5777–5794. [PubMed: 8795632]
- Landmesser LT. The acquisition of motoneuron subtype identity and motor circuit formation. *Int J Dev Neurosci* 2001;19:175–182. [PubMed: 11255031]
- Li X, McGinnis W. Activity regulation of Hox proteins, a mechanism for altering functional specificity in development and evolution. *Proc Natl Acad Sci U S A* 1999;96:6802–6807. [PubMed: 10359793]
- Liu JP, Laufer E, Jessell TM. Assigning the positional identity of spinal motor neurons: rostrocaudal patterning of Hox-c expression by FGFs, Gdf11, and retinoids. *Neuron* 2001;32:997–1012. [PubMed: 11754833]
- Livet J, Sigrist M, Stroebel S, De Paola V, Price SR, Henderson CE, Jessell TM, Arber S. ETS gene *Pea3* controls the central position and terminal arborization of specific motor neuron pools. *Neuron* 2002;35:877–892. [PubMed: 12372283]
- Maconochie M, Nonchev S, Morrison A, Krumlauf R. Paralogous Hox genes: function and regulation. *Annu Rev Genet* 1996;30:529–556. [PubMed: 8982464]
- McGinnis W, Krumlauf R. Homeobox genes and axial patterning. *Cell* 1992;68:283–302. [PubMed: 1346368]
- McIntyre DC, Rakshit S, Yallowitz AR, Loken L, Jeannotte L, Capecchi MR, Wellik DM. Hox patterning of the vertebrate rib cage. *Development* 2007;134:2981–2989. [PubMed: 17626057]
- Nordstrom U, Maier E, Jessell TM, Edlund T. An early role for WNT signaling in specifying neural patterns of Cdx and Hox gene expression and motor neuron subtype identity. *PLoS Biol* 2006;4:e252. [PubMed: 16895440]
- Prasad A, Hollyday M. Development and migration of avian sympathetic preganglionic neurons. *J Comp Neurol* 1991;307:237–258. [PubMed: 1713232]
- Rinn JL, Kertesz M, Wang JK, Squazzo SL, Xu X, Bruggmann SA, Goodnough LH, Helms JA, Farnham PJ, Segal E, et al. Functional demarcation of active and silent chromatin domains in human HOX loci by noncoding RNAs. *Cell* 2007;129:1311–1323. [PubMed: 17604720]
- Ronshaugen M, Biemar F, Piel J, Levine M, Lai EC. The *Drosophila* microRNA *iab-4* causes a dominant homeotic transformation of halteres to wings. *Genes Dev* 2005;19:2947–2952. [PubMed: 16357215]
- Rouso DL, Gaber ZB, Wellik D, Morrisey EE, Novitch BG. Coordinated actions of the forkhead protein *Foxp1* and Hox proteins in the columnar organization of spinal motor neurons. *Neuron* 2008;59:226–240. [PubMed: 18667151]
- Schuettengruber B, Cavalli G. Recruitment of polycomb group complexes and their role in the dynamic regulation of cell fate choice. *Development* 2009;136:3531–3542. [PubMed: 19820181]
- Shah V, Drill E, Lance-Jones C. Ectopic expression of *Hoxd10* in thoracic spinal segments induces motoneurons with a lumbosacral molecular profile and axon projections to the limb. *Dev Dyn* 2004;231:43–56. [PubMed: 15305286]
- Shen WF, Rozenfeld S, Lawrence HJ, Largman C. The Abd-B-like Hox homeodomain proteins can be subdivided by the ability to form complexes with *Pbx1a* on a novel DNA target. *J Biol Chem* 1997;272:8198–8206. [PubMed: 9079637]
- Shirasaki R, Pfaff SL. Transcriptional codes and the control of neuronal identity. *Annu Rev Neurosci* 2002;25:251–281. [PubMed: 12052910]
- Smith CL, Hollyday M. The development and postnatal organization of motor nuclei in the rat thoracic spinal cord. *J Comp Neurol* 1983;220:16–28. [PubMed: 6315781]

- Sockanathan S, Jessell TM. Motor neuron-derived retinoid signaling specifies the subtype identity of spinal motor neurons. *Cell* 1998;94:503–514. [PubMed: 9727493]
- Soshnikova N, Duboule D. Epigenetic temporal control of mouse Hox genes in vivo. *Science* 2009;324:1320–1323. [PubMed: 19498168]
- Tarchini B, Huynh TH, Cox GA, Duboule D. HoxD cluster scanning deletions identify multiple defects leading to paralysis in the mouse mutant Ironside. *Genes Dev* 2005;19:2862–2876. [PubMed: 16322559]
- Trainor PA, Krumlauf R. Patterning the cranial neural crest: hindbrain segmentation and Hox gene plasticity. *Nat Rev Neurosci* 2000;1:116–124. [PubMed: 11252774]
- Tsuchida T, Ensini M, Morton SB, Baldassare M, Edlund T, Jessell TM, Pfaff SL. Topographic organization of embryonic motor neurons defined by expression of LIM homeobox genes. *Cell* 1994;79:957–970. [PubMed: 7528105]
- Tumpel S, Wiedemann LM, Krumlauf R. Hox genes and segmentation of the vertebrate hindbrain. *Curr Top Dev Biol* 2009;88:103–137. [PubMed: 19651303]
- van der Lugt NM, Alkema M, Berns A, Deschamps J. The Polycomb-group homolog Bmi-1 is a regulator of murine Hox gene expression. *Mech Dev* 1996;58:153–164. [PubMed: 8887324]
- Vermot J, Schuhbauer B, Le Mouellic H, McCaffery P, Garnier JM, Hentsch D, Brulet P, Niederreither K, Chambon P, Dolle P, et al. Retinaldehyde dehydrogenase 2 and Hoxc8 are required in the murine brachial spinal cord for the specification of Lim1+ motoneurons and the correct distribution of Islet1+ motoneurons. *Development* 2005;132:1611–1621. [PubMed: 15753214]
- Wellik DM. Hox genes and vertebrate axial pattern. *Curr Top Dev Biol* 2009;88:257–278. [PubMed: 19651308]
- Wichterle H, Lieberam I, Porter JA, Jessell TM. Directed differentiation of embryonic stem cells into motor neurons. *Cell* 2002;110:385–397. [PubMed: 12176325]
- Wu Y, Wang G, Scott SA, Capecchi MR. Hoxc10 and Hoxd10 regulate mouse columnar, divisional and motor pool identity of lumbar motoneurons. *Development* 2008;135:171–182. [PubMed: 18065432]

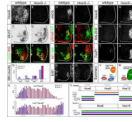


Figure 1. Transformation of Columnar Identities in *Hoxc9* Mutants

(A–B) Loss of Hoxc9 protein at thoracic levels in *Hoxc9* mutants. Sections show ventral right quadrant of e11.5 spinal cord. (C–F) Expression of *VAcHt* and the number of *Lhx3*⁺*Hb9*⁺ MMC MNs are grossly normal in *Hoxc9* mutants. (G) Quantification of MN columnar subtypes (n>3 mice, error bars represent SEM). In *Hoxc9* mutants total MN number at thoracic levels is increased ~30%, approximating limb-level numbers (data not shown). (H–K) Loss of nNOS and pSmad expression in *Hoxc9* mutants. (L–O) In the absence of Hoxc9, the number of *Isl1/2*⁺ *Hb9*⁺ MNs is reduced and *Er81* is not detected. (P–U) Ectopic *Hoxc6*, *RALDH2*, and *FoxP1*^{high} MNs at thoracic levels in *Hoxc9* mutants. (V–W) Schematic representation of thoracic MN columnar subtypes in wildtype and *Hoxc9* mutants. Motor neuron markers for profiling are shown. (X) Quantification of *FoxP1*⁺*Hoxc6*⁺ and *FoxP1*⁺*RALDH2*⁺ LMC MNs along the rostrocaudal axis at e11.5. Results show cell counts for one embryo that are typical of n>5 animals. *FoxP1* counts represent ventral lateral MNs that express high levels. (Y) Summary of MN columnar transformations in *Hoxc9* mutants.

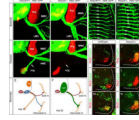


Figure 2. Altered Motor Axon Projection Patterns in *Hoxc9* Mutants

(A–D) Vibratome sections showing motor axon projections in wildtype and *Hoxc9* mutant embryos at e13.5. (A–B) Axonal projections at brachial levels in wildtype and *Hoxc9* mutants. Projections to limb (LMC) and axial muscles (MMC) are preserved. (C–D) In *Hoxc9* mutants, axonal projections to sympathetic chain ganglia (scg) are significantly reduced at e13.5 (arrows). See also Figure S3. Vibratome sections show GFP⁺ motor axons in green, Isl1/2⁺ scg and dorsal root ganglion (drg) neurons in red. (E–F) Schematic representations of axonal projections of thoracic MNs in wildtype and *Hoxc9* mutants. (G–H) The thickness of the intercostal nerves is increased in *Hoxc9* mutants (white bars). (I–N) Retrograde labeling of MNs after rhodamine (RhD) injection into intercostal nerves. Ectopic FoxP1^{high} LMC neurons are labeled in *Hoxc9* mutants, while Lhx3⁺ MMC MNs are not labeled.

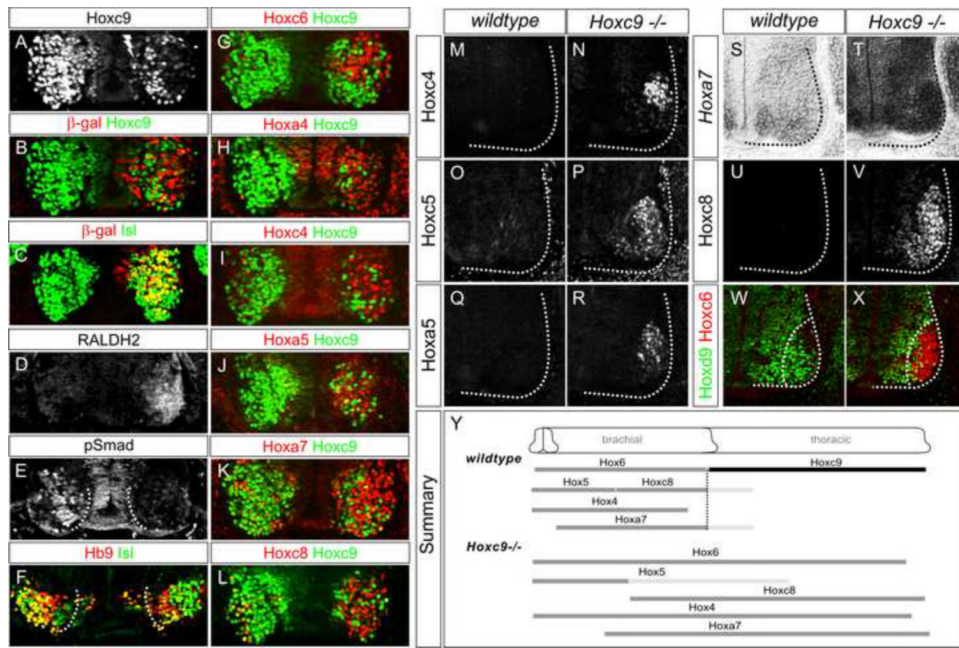


Figure 3. Cell Autonomous Role of Hoxc9 in MN Fate and *Hox* Gene Expression

(A–L) Analysis of Hoxc9 knockdown at thoracic levels after dsRNA electroporations in chick neural tube. Bolt indicates electroporated side. (A) *Hoxc9* dsRNA reduces Hoxc9 protein expression. (B) Nuclear LacZ expression plasmid was coelectroporated to mark electroporated cells. Note that the LacZ plasmid labels only a fraction of cells that incorporate the dsRNA. (C) *Hoxc9* dsRNA does not affect *Isl1/2* expression. (D) Ectopic RALDH2 is detected after thoracic Hoxc9 RNAi. (E) Loss of pSmad expression. (F) The number of Hb9⁺Isl1/2⁺ HMC neurons is reduced after Hoxc9 removal. (G–L) Hoxc6, Hoxa4, Hoxc4, Hoxa5, Hoxa7, and Hoxc8 are ectopically expressed or upregulated in cells that have lost Hoxc9. (M–V) Derepression of Hoxc4, Hoxc5, Hoxa5, Hoxa7, and Hoxc8 expression at thoracic levels in *Hoxc9* mutants. The normal brachial patterns of *Hox* genes were intact in *Hoxc9* mutants (Figure S4A–S4H). Ectopic Hox5 expression was relatively weak at thoracic levels, possibly due to the presence of Hoxc8 which normally restricts *Hox5* genes to rostral brachial MNs (Dasen et al., 2005). (W–X) Loss of Hoxd9 expression in MNs that ectopically express Hoxc6. (Y) Summary indicating brachially-restricted *Hox* genes that are ectopically expressed or upregulated in *Hoxc9* mutants. Light-gray bars indicated reduced protein expression levels.

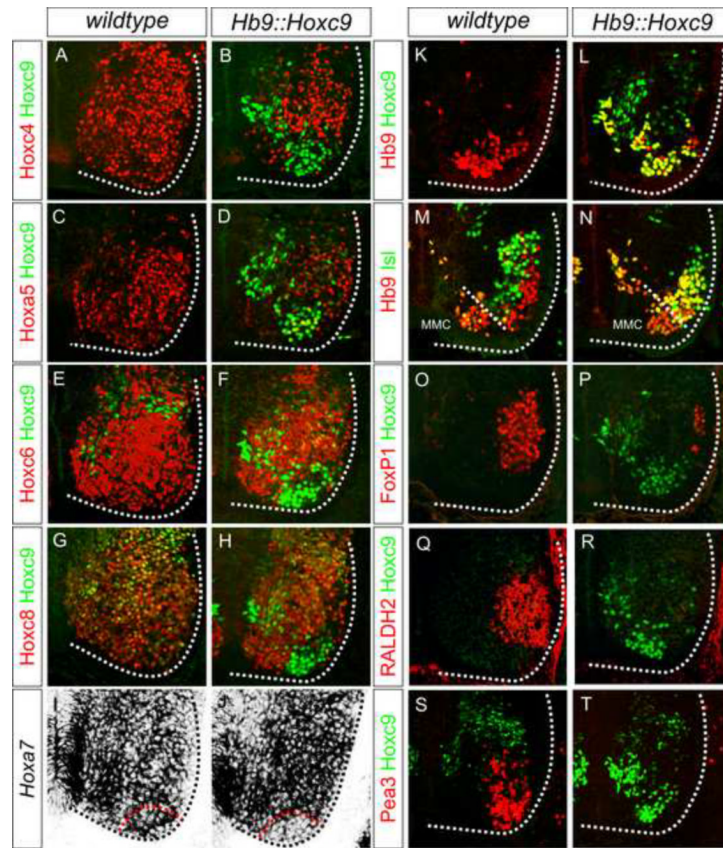


Figure 4. Hoxc9 Represses Brachial *Hox* Genes and LMC Identity

(A–J) Brachial analysis of *Hox* profiles and motor neuron fates in e12.5 *Hb9::Hoxc9* embryos. *Hoxc4*, *Hoxa5*, *Hoxc6*, *Hoxc8*, and *Hoxa7* expression are repressed or significantly downregulated by *Hoxc9* in brachial MNs. *Hox* expression is preserved in the surrounding ventral interneurons. Red dashed line in panel (J) outlines region where *Hoxc9* is misexpressed and corresponding region in control mice (I). (K–L) *Hb9*⁺ *Hoxc9*⁺ MNs are generated in *Hb9::Hoxc9* transgenic mice. (M–N) The number of *Hb9*⁺*Isl1*⁺/*Isl2*⁺ neurons is increased in *Hb9::Hoxc9* transgenic mice. In the absence of a *Hox*-induced program, MNs appear to remain in a HMC-like ground state. (O–R) *Hoxc9* expression in brachial MNs reduces the number of *FoxP1*⁺ and *RALDH2*⁺ LMC MNs. (S–T) *Hoxc9* expression blocks expression of the motor pool marker *Pea3*.

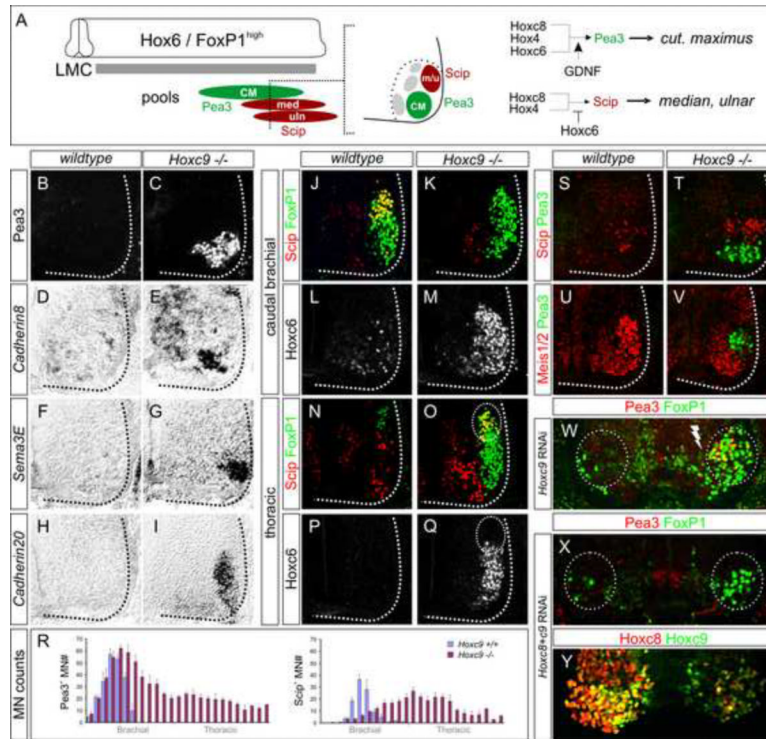


Figure 5. Motor Pool Reorganization in *Hoxc9* Mutants

(A) Schematic of the combinatorial Hox codes for motor pools at caudal brachial levels of the spinal cord. Pea3 marks cutaneous maxims (CM) MNs, Scip marks median (med) and ulnar (uln) MNs. Scip MNs are present at the most caudal brachial regions and require exclusion of Hoxc6. (B–I) Multiple markers of the CM pool are detected at thoracic levels in *Hoxc9* mutants. The normal brachial patterns were preserved (Figure S6A–S6B and S6I–S6N). (J–M) At caudal brachial levels, upregulation of Hoxc6 expression in *Hoxc9* mutants is accompanied by loss of brachial Scip LMC MNs. (N–Q) Altered position of the Scip pool. In *Hoxc9* mutants Scip is expressed at thoracic levels. Ectopic Scip neurons are also detected in *Hoxc9* RNAi ablated embryos (Figure S6S–S6T). (R) Cell counts for Pea3 and Scip MNs in wildtype and *Hoxc9* mutants. Error bars represent $n > 3$ *Hoxc9* mutants. (S–T) Ectopic Scip⁺ and Pea3⁺ MNs at thoracic levels are clustered normally in *Hoxc9* mutants. (U–V) Expression of Meis1/2 is excluded from the Pea3 pool. (W) Pea3 is ectopically expressed at thoracic levels after *Hoxc9* RNAi. Bolt: electroporated side. (X) Knockdown of both *Hoxc8* + *Hoxc9* by dsRNA show that ectopic LMC neurons (FoxP1^{high}) fail to generate ectopic Pea3 at thoracic levels. (Y) Loss of both Hoxc8 and Hoxc9 proteins after coelectroporation of dsRNAs.

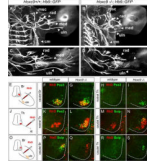


Figure 6. Altered Limb Innervation Patterns in *Hoxc9* Mutants

(A–D) Forelimb innervation in *Hoxc9*^{+/+}; *Hb9*::*GFP* and *Hoxc9*^{-/-}; *Hb9*::*GFP* embryos. Motor axons are visualized by whole mount GFP staining. (A–B) At e12.5 both ulnar (uln) and median (med) nerves show a reduction in length in *Hoxc9* mutants. Musculocutaneous (mus), radial (rad), and cutaneous maximus (cm) nerves are similar to wildtype in *Hoxc9* mutants. See also Figure S7G–S7J. (C–D) At e13.5 the density of ulnar projections are reduced and there is a loss of the distal branch of the median nerve in *Hoxc9* mutants. (E–I) Labeled MNs after RhD injection into the CM nerves. RhD labels the normal *Pea3* domain at caudal brachial levels in *Hoxc9* mutants. (J–N) Ectopic *Pea3* and *Scip* are labeled after RhD injection into the intercostal nerves at thoracic levels in *Hoxc9* mutants. (O–S) In *Hoxc9* mutants RhD labels scattered *Scip*⁻ cells at caudal brachial region, but not ectopic *Scip*⁺ cells present at thoracic levels after ulnar injection.

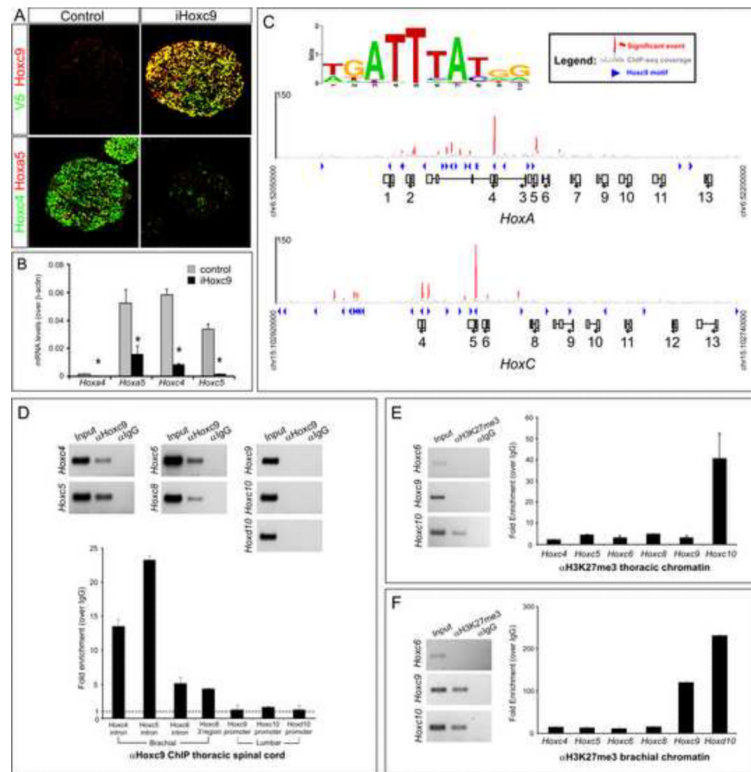


Figure 7. Genomic Analysis of Hoxc9 Binding at *Hox* Loci in Motor Neurons
 (A) Immunostaining showing induction of epitope (V5)-tagged Hoxc9 in embryonic bodies represses Hoxc4 and Hoxa5 expression. (B) RT-PCR analysis of *Hoxa4*, *Hoxa5*, *Hoxc4*, and *Hoxc5* transcripts in control and Hoxc9 induced (iHoxc9) ES-cell derived MNs. (C) ChIP-seq signal maps for Hoxc9 binding sites within the *Hox-a* and *Hox-c* loci. Hoxc9 consensus motifs are indicated by blue arrowheads and significant binding events are shown in red peak. (D) Hoxc9 binds anterior *Hox* gene regions at thoracic levels *in vivo*. Top panels show gel images and bottom panels RT-PCR analysis from ChIP assays. Potential binding sites of *Hox* genes were assessed by ChIP using Hoxc9 specific antibody. Binding of Hoxc9 to the *Hoxa7* 3' region was not detected, possibly due to reduced sensitivity of *in vivo* ChIP assay. Error bars represent standard deviation on triplicates. (E) H3K27me3 chromatin status at *Hox* gene promoters at thoracic levels (F) H3K27me3 status of *Hox* gene promoters at brachial levels.

